DOI: 10.1002/asia.200800298

Colloidal Lithography—The Art of Nanochemical Patterning

Gang Zhang[a] and Dayang Wang*[b]

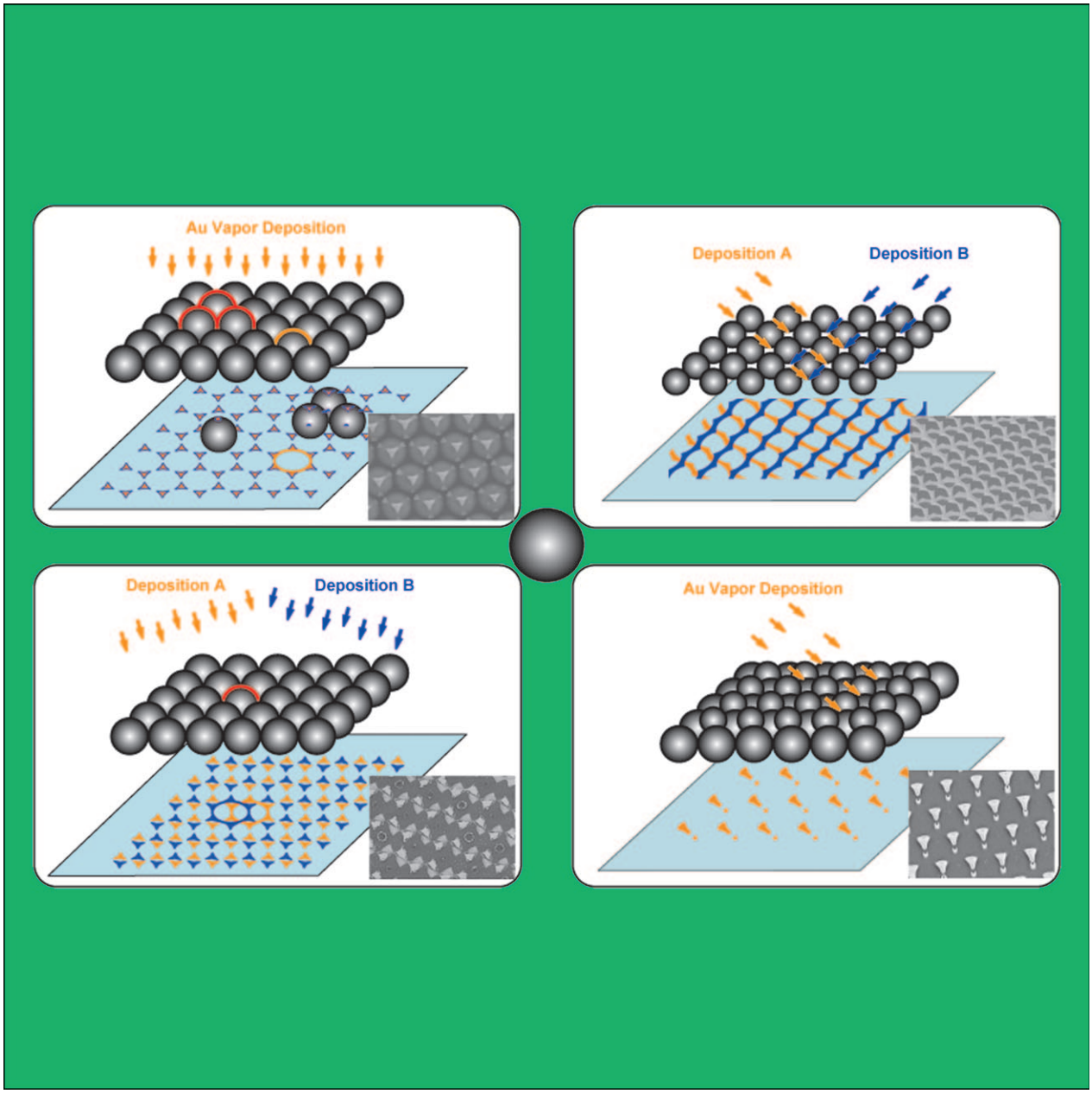

Abstract: Colloidal lithography relies on using colloidal crystals as masks for etching and deposition, and allows fabrication of various nanostructures on planar and non-planar substrates with low-cost, high-throughput-processing, large fabrication area, and a broad choice of materials. The feature size can easily shrink by decreasing the microsphere diameter in the colloidal mask. The feature shape can be diversified by varying the crystal structure of the colloidal mask, etching the mask, altering the incidence angle of the vapor beam, and stepwise manipulation of the mask registry. This nanochemical patterning strategy paves a complementary way to conventional top-down lithography. This focus review provides an overview of the principle of colloidal lithography, and surveys the recent developments as well as outlining the future challenges.

Keywords: colloids · lithography · nanostructures · patterning · self-assembly

1. Introduction

Lithography—stone-writing in Latin—is one of several terms shared by both scientists and artists. Since it was invented by Alois Senefelder in 1798, it was rapidly developed to be an efficacious tool for the printing of pictures and exotic characters, for example, and, at the same time, be a popular artistic medium for printmaking. Since the 1950s, when gum arabic was replaced by a resist, limestones replaced by silicon wafers, and the design and replication of a pattern onto a substrate done by using high energy beams such as light, lithography has provided an ingenious and powerful way to fabricate micro- or nano-structures for making integrated circuits and microelectromechanical systems. In semiconductor manufacturing, lithography goes far beyond a planographic process in an atelier. Artists prefer to call lithography a "chemical process" because for them, the chemical interaction between gum arabic, nitric acid, grease, water, and limestone is rather complicated when compared to the drawing of patterns. Although a more complicated chemical process is embodied during design, preparation, and transfer of a pattern, the success of lithography as a microfabrication tool is determined by the capability of creating a pattern with high resolution and high precision on a micrometer or nanometer scale.

[a] Dr. G. Zhang
State Key Lab of Supramolecular Structure and Materials
College of Chemistry, Jilin University
130012, Changchun (P.R. China)

[b] Dr. D. Wang
Max Planck Institute of Colloids and Interfaces
14424 Potsdam (Germany)
Fax: (+49) 331-567-9202
E-mail: dayang.wang@mpikg-golm.mpg.de

For the past few decades, a number of new lithographic techniques have been successfully developed, including photolithography, tow-photon-lithography, holographic lithography, molding and imprinting, scanning probe nano-machining, electron beam lithography, ion beam lithography, and dip-pen writing and the variants thereof.[1–10] All these techniques can be classified into two categories, mask-assisted lithography and maskless lithography. Using a high-energy beam or a rigid stylus to etch or cut a substrate is a straightforward process of writing two dimensional (2D) and even three dimensional (3D) patterns.[7–10] Maskless lithographic techniques are a pixel-by-pixel and voxel-by-voxel fabrication process and require sophisticated, expensive, and, in most cases, cumbersome apparatuses, for instance, for the genesis of energetic particles. As such, they are expensive, slow, have low-throughput, and only suitable for patterning on very small areas. Mask-assisted lithography is, in nature, the same as lithographic printmaking. The process starts with the design of a pattern in the form of a mask, which is subsequently used for template etching of a substrate with a reasonably high throughput.[4–6] To date, mask-assisted lithographic techniques, especially photolithography and its variants, remain the major workhorse for patterning. As compared with maskless techniques, most mask-assisted lithographic techniques are limited to 2D patterning. Its flexibility is limited to a large extent by the cost, difficulty, and delay associated with the design and preparation of a pattern for use as a mask having a high resolution on a micrometer or nanometer scale.

The advent of nanoscience and nanotechnology has led to tremendous enthusiasm from researchers from different scientific disciplines, such as physics, chemistry, and biology, to engage with nanostructures with the intent of pursuing the innovative properties derived in the nanometer dimen-

sion.[11–14] In this context, the fabrication of nanostructures becomes the escalating demand. Obviously, the low-throughput and expensive maskless lithography is a less attractive choice for chemists, physicists, material scientists, and biologists. The success of extending mask-assisted lithography beyond microelectronics workshops is also largely limited by mask design and preparation. Furthermore, conventional lithographic techniques work well for semiconductor materials and photoresists, yet show difficulty for introducing specific chemical functionality. To pattern non-planar surfaces is also difficult. Recently, a tremendous effort has been devoted to develop non-conventional lithographic techniques especially integrated with a bottom-up nanochemical procedure.[3,15] One of the most attractive non-conventional lithographic techniques is soft lithography, which uses an elastomer stamp or mold to pattern various substrates with the aid of self-assembly of organic molecules in an ambient lab environment.[16] It allows easy patterning of large area, planar and curved surfaces exhibiting a high resolution on a nanometer scale. However, soft lithography still requires an assistance of conventional mask-assisted lithographic techniques, such as photolithography, to design and make a patterned elastomer master. To develop ingenious, cheap, and non-lithographic ways to make masks or masters with high resolution (below 100 nm), a great deal of self-assembly nanostructures have been recruited for masking, including laterally structured Langmuir–Blodgett monolayers, liquid crystalline structures of amphiphilic surfactants, microphase separation structures of block copolymers, and self-assembly of proteins and nanoparticles.[17–21]

Monodisperse microspheres with sizes ranging from tens of micrometers to tens of nanometers, can easily be synthesized by conventional emulsion polymerization or sol-gel synthesis techniques. Owing to the size and shape monodispersity, they can self-assemble into a 2D and 3D extended periodic array, coined as a colloidal crystal.[22–25] During the past few decades, the emergence of photonic crystals has initiated the explosion for studying the creation of 3D colloidal crystals and using them to template the formation of macroporous structures in order to pursue a complete 3D photonic bandgap. Prior to the enthusiasm shown for growing 3D inverted macroporous structures, the interstitial array in a colloidal crystal was used as a mask for etching or deposition to create 2D patterns on a substrate. This patterning process is preferentially referred to as colloidal lithography (CL), paving a simple and low-cost for patterning with a flexibility of scaling down the feature size below 100 nm.

Abstract in Chinese:

胶体刻蚀是以胶体晶体为模板进行刻蚀或沉积，能够在平面或曲面基材上构造多种纳米结构，具有低成本、高产出、大面积以及材料选择范围宽等特点。单元尺寸可以通过缩小胶体模板微球的直径进行简单控制。单元形状的控制可以通过改变胶体模板的晶体结构、模板的刻蚀、改变沉积气体流入射角度以及控制胶体模板的方位角度来实现。这种纳米化学图案化策略为传统的“自上而下”图案化提供了一种补充。本文概述了胶体刻蚀的基本原理，纵览了近期的发展，并勾勒出未来的挑战。

2. Colloidal Lithography

2.1. In retrospect

To the best of our knowledge, the periodical array of a close-packed microsphere monolayer was first used as a mask for the deposition of platinum in 1981 by Fischer and Zingsheim.[26] Soon after, Deckman and co-workers successfully extended this technique for large area surface patterning, and called it “natural lithography”.[27–29] The word “natural” comes from the fact that the masks were obtained by self-assembly of colloidal microspheres rather than by photolithography. They have also pioneered the work of etching a colloidal crystal into a textured surface using a reactive ion beam.[28] Van Duyne and co-workers have undertaken numerous efforts to develope patterning techniques that use colloidal crystals as masks for metallic vapor deposition.[30–33] In the context of nanoscience, they changed the name of CL from natural lithography to nanosphere lithography. They

Gang Zhang was born in Mudanjiang, China in 1972. He obtained his PhD in polymer chemistry and physics at Jilin University, Changchun, China in 2003. He worked as an assistant and lecturer at Jilin University from 1997 to 2003, and he was a postdoctoral fellow at Max Planck Institute of Colloids and Interfaces, Potsdam, Germany from 2003 to 2006. He is now an associate professor at Jilin University and his research interests include ordered micro- and nanostructures and applications, heterogeneous asymmetric structure and assembly, colloidal and interface assembly.

Dayang Wang studied chemistry at Jilin University, Changchun, P.R. China where he received a PhD degree in polymer chemistry and physics in 1998. In 1999, he moved to the Max Planck Institute of Colloids and Interfaces (MPIKG), Potsdam, Germany, as a postdoctoral fellow. In 2000, he received an Alexander von Humboldt fellowship at MPIKG. He is now a group leader at MPIKG and his research focuses on fabricating colloidal particles with unusual geometric and chemical symmetries and supervising them to self-assemble into nanostructures with defined dimensions, complexities, and functions.

explored how to use various experimental parameters, especially the incident angle to diversify the patterns obtained. Furthermore, they also succeeded in extending the single layer masking to double layer masking. Of most importance is that they have intensively investigated the plasmon resonance properties of metallic patterns obtained by CL and drew a correlation with the feature morphology, with the intent of developing highly-sensitive biosensors based on surface enhanced Raman spectroscopy.[34–35] Following the seminal work of Van Duyne and co-workers, colloidal crystals are now recognized as low-cost, flexible, and easily adoptable masks for growing new nanostructures with diverse structural complexity.

The present article centers on reviewing the new developments of CL to underline the impact of CL on surface patterning using the most recent results, from our research group and others, as a basis. We apologize to the authors of excellent work since, owing to the diverse activity in this field, their work has unintentionally been left out. We commence with the creation of complicated patterns on planar substrates. The following section outlines the new development of using a modified CL process to create complicated patterns on microspheres. Finally, a conclusive remark and outlook will be given, discussing the advantages and disadvantages of CL and the future challenges entailed.

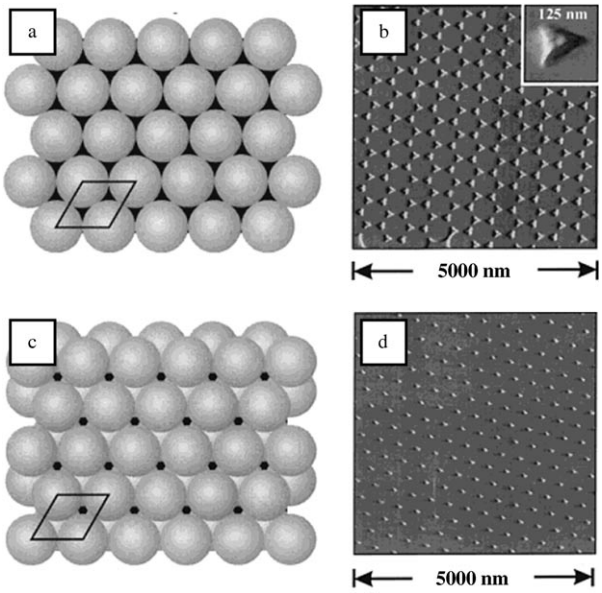

Figure 1. Schematic illustration (a) and representative atom force micrograph (AFM) (b) of nanodots derived from CL using an hcp single layer as a mask for deposition. The microspheres are 542 nm in diameter. The thickness of silver dots is 48 nm. Schematic illustration (c) and representative AFM (d) of nanodots derived from CL using an hcp double layer as a mask for deposition. The microspheres are 400 nm in diameter. The thickness of silver dots is 30 nm. Reprinted with permission.[32]

2.2. Patterning of Planar Substrates

2.2.1. Colloidal Crystal Masking.

Monodisperse microspheres, such as polystyrene (PS) or silica, readily self-assemble to single layers and multilayers with a hexagonal close-packing (hcp) array, which can be driven simply by the capillary force arising from solvent evaporation.[22–25] Recently, a host of colloidal crystallization strategies have been successfully established, including vertical deposition,[36] dip-coating,[37] spin-coating,[38,39] nano-robotic manipulation,[40] template-assisted epitaxial growth,[41,42] and crystallization driven by depletion force,[43] both at the water/air interface,[44,45] and within physically confined compartments[46]. Between the solid spheres in a colloidal crystal are interstices that are arranged into an ordered structure, inverted to the ordered structure of the solid spheres. When a colloidal crystal is used as a mask for deposition, the vapor beam can reach the substrate only through the interstices between the spheres, and the shape of the nanodots deposited on the substrate is determined by the projection shape of the interstices on the substrate (Figure 1 a). The interstices in an hcp single layer of microspheres have quasi-triangular projections arranged with P6mm symmetry on a substrate, so an array of P6mm arranged triangular metal dots is derived from the single masking after deposition and removal of the mask (Figure 1 b). The feature size is about a quarter of the sphere diameter and the distance between nearest-neighbor dots is around half of the sphere diameter. When an hcp double layer is used as a mask, the overlapping of the interstices between the upper and lower layers leads to a hexagonal array of quasi-hexagonal projection on a substrate, thus yielding a hexagonal array of quasi-hexagonal nanodots (Figures 1 c and 1 d).

In order to diversify the interstitial structure in a colloidal crystal, a number of post treatment methods have been employed to deform the constituent spheres. Latex microspheres can swell in an organic solvent, or deform when the environmental temperature is above their glass transition temperature. Recently swelling with the assistance of heating by, for instance, microwave has been used to shrink the interstice size in colloidal crystals (Figure 2).[47] Using reactive ion beams to machine an organic or inorganic colloidal crystal, leads to anisotropic etching of the constituent spheres because the upper layers act as shadow masks for the lower layers during etching.[28,48,49] Using this anisotropic etching, Yang and co-workers have created very complicated interstitial textures, and the feature geometry can be controlled by the etching time and the layer numbers of a colloidal crystal (Figure 3).[48,49]

2.2.2. Incident Angle-Resolved Colloidal Lithography

Using a colloidal crystal as a mask, a number of techniques such as thermal evaporation, sputtering deposition, electrochemical deposition, chemical vapor deposition, and so on, have been used to create patterns of inorganic (e.g., gold) and organic materials (e.g., cobalt phthalocyanine[30]). Marks and co-workers have succeeded in creating a periodic array of nanoscale organic light-emitting diodes, referred to as nanodiodes, by means of CL, enabling a shortcut to an opto-

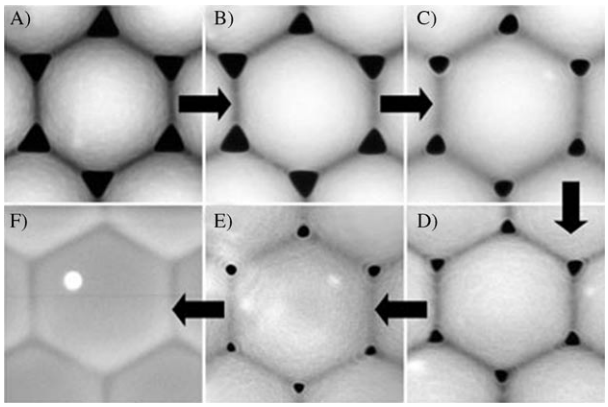

Figure 2. A 540 nm PS latex mask annealed in 25 mL of water/EtOH/acetone mixture by A) 1, B) 2, C) 4, D) 6, E) 7, and F) 10 microwave pulses. Reprinted with permission.[47]

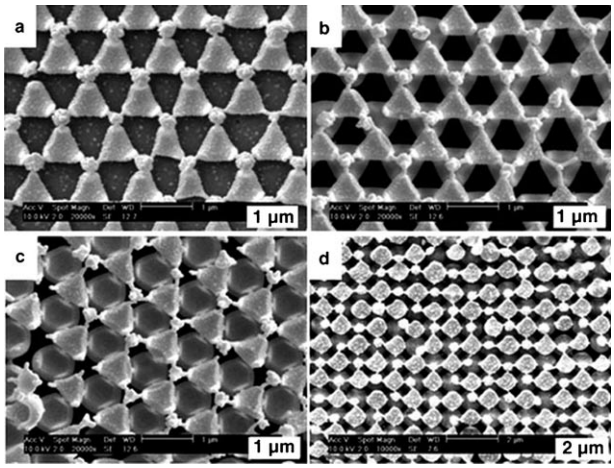

Figure 3. Modification of a mask using RIE for the fabrication of binary and ternary particle arrays with nonspherical building blocks. (a) and (b) Triangle arrays using binary and ternary colloidal spheres with an hcp arrangement. (c) and (d) Polygonal structures produced from colloidal layers with the (111) plane and the (100) plane of the face-centered-cubic structure, respectively. Reprinted with permission.[49]

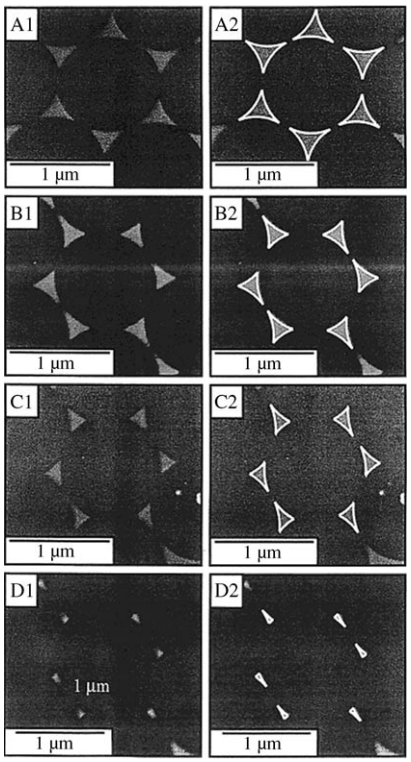

Figure 4. Field emission SEM images of ARCL fabricated - gold nanodot arrays and images with simulated geometry superimposed, respectively. (A1, A2) $\theta = 10°$, $\phi = 28°$, (B1, B2) $\theta = 20°$, $\phi = 2°$, (C1, C2) $\theta = 26°$, $\phi = 16°$, and (D1, D2) $\theta = 40°$, $\phi = 2°$. All samples are Cr deposited onto Si-(111) substrates. Images were collected at 40k magnification. θ is the incidence angle and ϕ the azimuth angle. Reprinted with permission.[33]

electronic device.[50] The deposition is usually conducted in a line-of-sight fashion, that is, the substrate coated with a colloidal crystal mask is positioned normal to the propagation direction of a material vapor. As such, the nanodots deposited on a substrate have an in-plane triangular or hexagonal shape, depending on the layer number of the template colloidal crystal (Figure 1).

Van Duyne and co-workers pioneered angle-resolved colloidal lithography (ARCL), that is, deposition of materials at the non-zero incident angle (θ) of the vapor beam with respect to the normal direction of the substrate.[31–32] Van Duyne et al. have used an hcp single layer as a mask. This angle resolved patterning not only reduced the dimension of the resulting nanodots by a factor of 4 but also deformed the shape from an equilateral to an isosceles triangle (Figure 4).[33] Furthermore, other new nanostructures, such as nanooverlaps, nanocontacts, nanogaps, and nanochains, have been created, exhibiting diverse optical characteristics.[32] Lee and co-workers have created arrays of nanodots having the shape of a crescent moon with a sub-10 nm sharp edge, which can enhance the local electromagnetic field at the edge.[51] Giersig and co-workers present a variant of ARCL, rotating the sample holder during vapor deposition at a non-zero incident angle.[47,52] Following the new strategy, they have created magnetic nanoring arrays with P6mm symmetry using hcp microsphere single layers as the mask (Figure 5).[47]

Recently, a stepwise strategy has successfully been developed to conduct ARCL.[52–54] We have used an hcp single layer of microspheres as a mask to deposit gold at $\theta = 15°$, and silver at $\theta = -15°$. After removal of the colloidal mask, a regular binary array comprising of identically-sized gold and silver nanodots alternatively arranged in a P6mm symmetry have been obtained (Figure 6).[53] Since each step of ARCL is independent of the chemical nature of the deposited materials, one can deposit any combination of materials into a regular binary array at will. Such heterogeneous binary arrays are hard to construct by conventional lithographic techniques. The feature morphology of the resulting binary array, however, shows a profound dependence on the registry of colloidal masks with respect to the incident vapor beam.

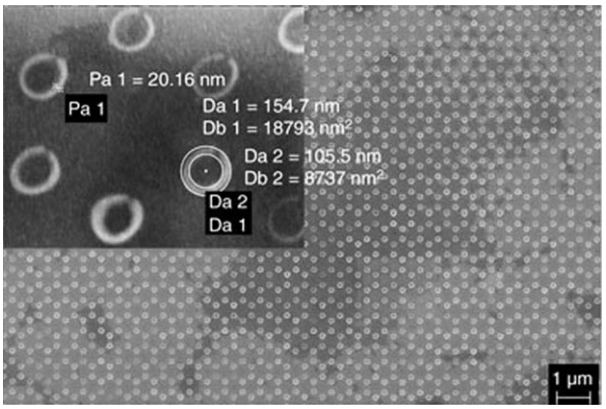

Figure 5. SEM picture of ordered Fe nanorings evaporated over an annealed 540 nm PS latex mask. The outer diameter of the single ring is 150 nm and the width of the ring is 20–30 nm. Reprinted with permission.[47]

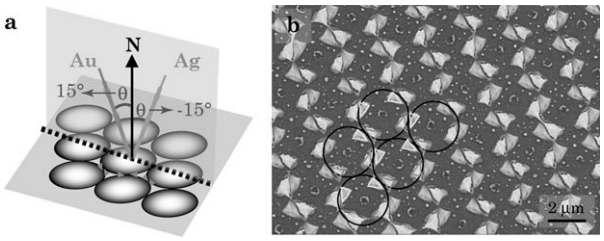

Figure 6. a) Schematic illustration of depositing gold and silver onto a hexagonally close-packed sphere monolayer at the incidence angles (θ) of 15 and −15°, respectively. The colloidal mask is registered so that the vector between nearest-neighbor spheres is in line with the projection of the incidence beam on the mask, highlighted by a black dotted line. b) SEM image of the resulting heterogeneous binary array. The mask is a monolayer of hexagonally close-packed 830 nm PS spheres. The original location of PS spheres, gold NPs, and silver NPs are highlighted by black circles, white triangles, and grey triangles, respectively. Reprinted with permission.[53]

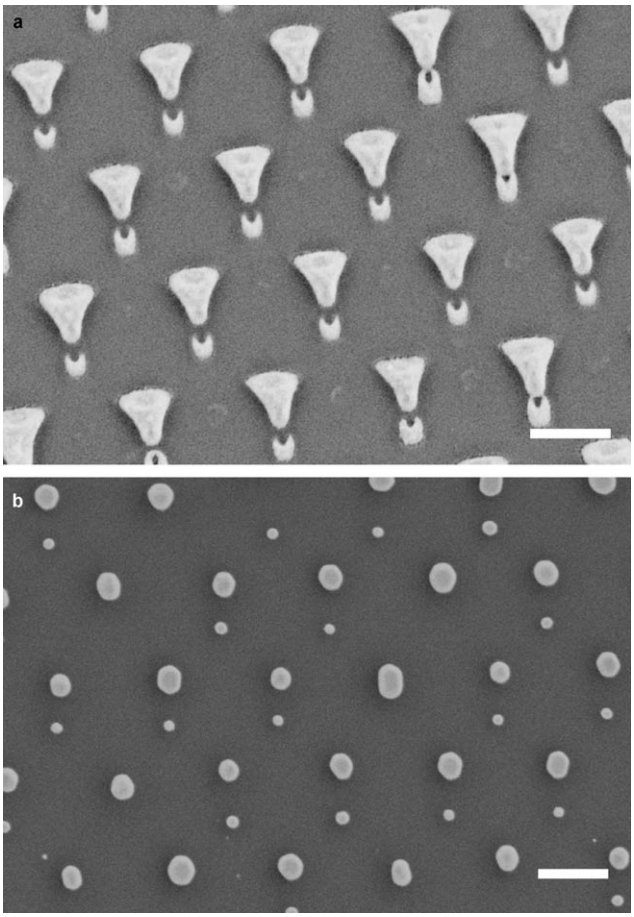

Figure 7. a) SEM picture of hexagonally arranged Au nanoshuttlecocks obtained by using double layers of hexagonal close-packed 830 nm PS spheres, etched by O_2 plasma for 10 min, as masks for Au vapor deposition at the incidence angel of 20°. b) SEM picture obtained after annealing the Au nanoshuttlecocks at 900 °C for 60 min. The scale bars are 500 nm. Reprinted with permission.[55]

ARCL is usually conducted using an hcp single layer of microspheres as a mask. Owing to the fact that the upper layer may shield the diffusion of the vapor beam and block the vapor propagation through the interstices in the lower layers, a double layer masking is rarely used for ARCL. To address this challenge, we used a reactive O_2 beam to etch an hcp double layer of PS microspheres prior to vapor deposition in order to reduce the size of the upper layer spheres and enlarge the interstices between them.[55] The use of the etched double layer as a mask allows deposition at varied θ values in the range of 15–45°. Following this modified double-layer-masked ARCL, a hexagonally arranged binary of large and small nanodots is obtained; the large nanodots are fan-shaped and the small ones crescent-shaped and they are, as a whole, shuttlecock-like (Figure 7a).[55] The gap between the large and small dot is expected, as a result of the shielding of the vapor propagation by the etched upper layer spheres. Distinct from the bulk materials, the nanoparticles have a much lower melting point that is very sensitive to the surface tension.[56] Habenicht and co-workers have demonstrated that the large curvature causes a higher surface tension and a lower melting point, and the annealing of non-round nanoparticles may give rise to a retraction of their apexes, and eventually generate a round shape.[57] Accordingly, we found that the post annealing treatment deformed the fan-shaped large dots and crescent-shaped small dots into large and small round dots, and the uniformity of the size and shape of the nanodots was dramatically improved (Figure 7b).[55]

2.2.3. Azimuth Angle-Resolved Colloidal Lithography

Van Duyne and co-workers have shown the significant role of the registry of colloidal crystal masks with respect to the propagation vector of the incident vapor beam during ARCL.[33] The difficulty in controlling the registry of the colloidal mask arises from the fact that the colloidal crystal mask is usually polycrystalline, yielding multiple hcp crystal domains that are randomly oriented. ARCL is usually limited to the small incidence angle, usually less than 30°.[33] The advance of colloidal crystallization technology, for instance

dip-coating,[37] spin-coating,[39] template-assisted epitaxy crystallization,[41,42] and crystallization on a floating substrate such as at the water/air interface,[45] enables one to grow a single crystalline hcp domain of microspheres over an area of 100 μm^2. Besides, it has been demonstrated that pre-reactive ion etching can reduce the non-uniformity of the pattern feature arising from the vacancy and dislocation defects in a colloidal crystal mask. Recently we have integrated reactive ion etching into an ARCL process.[54] The registry of the colloidal crystal mask is defined by the azimuth angle (ϕ) of the projection of the vapor beam on a substrate with respect to the vectors between the microspheres in the mask. With the aid of scanning electron microscopy (SEM), the colloidal mask can register the azimuth angle so that the projection of the vapor beam on the substrate is coincident with the vector between the nearest-neighbor spheres, for instance. After an hcp monolayer of latex microspheres is etched by O_2 plasma, the subsequent vapor deposition leads to zigzag nanowires when θ is larger than 45° (Figure 8b).[54] According to the symmetry of a hexagonally non-close packed sphere monolayer, there exist three distinct vectors between the nearest-neighbor spheres and three between next-nearest-neighboring spheres (Figure 8a).[54] As such, regularly varying the azimuth angle by 120° leads to a highly ordered quasi-3D grid of nanowires; three nanowires cross each other at an angle of 120° (Figure 8c).[54] The independence of the chemical nature of materials for each step of ARCL allows one to freely create nanowires from different materials with step-wise deposition and stack them into quasi-3D and 3D multiplex grids with a defined vertical and especially lateral heterogeneity. Such nanostructures are hard to be realized by conventional lithographic techniques, and even soft lithographic techniques.

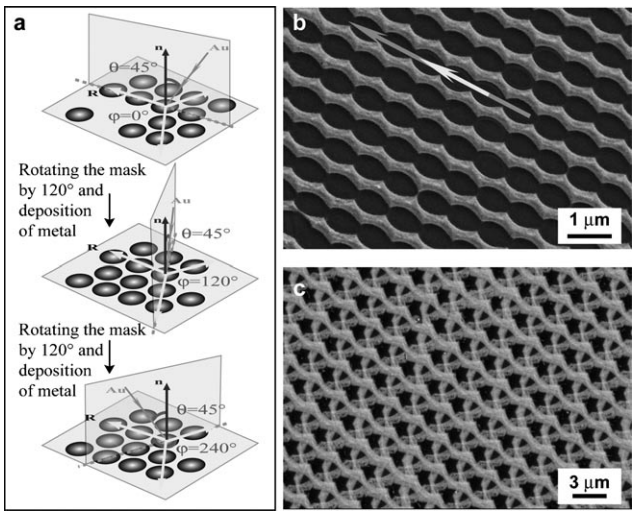

Figure 8. a) Schematic depiction of constructing quasi-3D grids of multiplex zigzag nanowires by stepwise rotating the colloidal mask by 120° with respect to the reference vector (R) between nearest-neighboring spheres over the course of metallic vapor deposition. The projection of metal vapor on the mask was set coincident with the reference vector (R), namely $\phi=0°$. The incidence angle (θ) is 45°. SEM images of quasi-3D grids of multiplex zigzag nanowires obtained by stepwise depositing gold, silver, and nickel at $\phi=0°$, $\phi=120°$, and $\phi=240°$ using plasma etched hcp single layers of 830 nm PS microspheres as masks. The plasma etching time is 20 min. The structure obtained by one and three deposition steps are show in (b) and (c), respectively. Reprinted with permission.[54]

2.3. Patterning on Microparticles

Contact printing with the aid of an elastomer stamp has demonstrated the flexibility to transfer the hcp monolayer of microspheres on a sticky substrate.[59–60] Colloidal crystallization has been easily extended to different substrates with various morphology, for instance on tubes[59] and in cavities.[61] Hence the colloidal crystal mask should offer an advantage for patterning non-planar substrates as commonly used lithographic masks. By taking the mechanical advantage of elastomer stamps or molds, soft lithography is capable of patterning non-planar substrates.[15,16] Nevertheless, it has difficulty to pattern the surface of a radius of curvature smaller than 50 μm. Using a two-axis-of-rotation drive system, Yamazaki and Namatsu have created a regular array of pillars of 100 nm in diameter on 25 μm poly(methylmethacrylate) spheres by electron beam lithography.[62] Patterning microspheres smaller than 25 μm remains a formidable challenge for conventional lithographic techniques.

Obviously, the surface of an hcp monolayer of microspheres offers a curved surface; the curvature is determined by the sphere radius. Albrecht and co-workers have demonstrated that the curved surface of an hcp microsphere monolayer can dramatically affect the magnetic properties of the materials deposited above.[63] Patterning on a microsphere dates from the late of 1990s with the intent of generating asymmetric particles—Janus particles—to mimic the interfacial behavior of amphiphilic molecules.[64–65] Theoretical modeling suggests that the anisotropic surface chemistry allows microspheres to self-assemble into exotic nanostructures that can be far away from the thermodynamically stable state.[66–68] Resulting from the lack of a proper mask for deposition or modification, only half the surface of a microsphere can be modified.[64–65,69–73]

In a colloidal crystal with a face-centered-cubic structure (ABCABC stacking) or hexagonal-close-packing structure (ABAB stacking), different layers are aligned precisely with respect to one another, and the spheres in the lower layer are positioned exclusively beneath the interstices in the upper layer. During the propagation of a vapor beam through the crystal, the upper layers are envisaged to offer a shadow mask effect and template deposition on the spheres in the lower layers. Taking this into account, we have recently developed a modified CL way to pattern the surfaces of microspheres.[74–76] By deposition of gold into an hcp double layer of microspheres, followed by peeling off the upper layer with a sticky stamp, various gold nanostructures are embossed on the microspheres in the lower layer. The feature shape, such as triangles, squares, and bowties, shows a pronounced correlation with the crystalline structure of the double layer mask (Figure 9).[74] The deposition condition,

CHEMISTRY
AN ASIAN JOURNAL

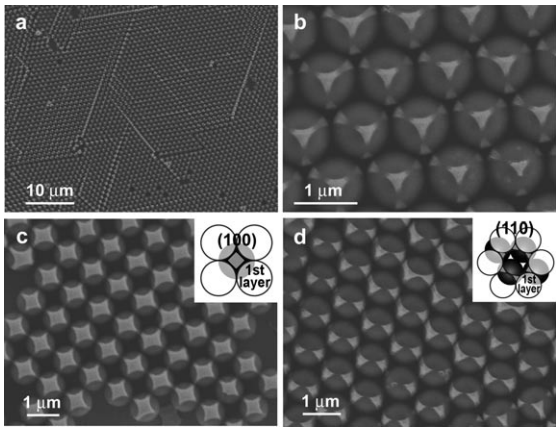

Figure 9. Low (a) and high (b) magnification SEM picture of 925 nm polystyrene spheres with gold patterned surfaces generated by templating the top monolayers of colloidal crystals with (111) facets parallel to the substrates. (c) and (d) SEM pictures of 925 nm polystyrene spheres with Au-patterned surfaces generated by using the top monolayers of colloidal crystals with preferential crystal orientation: (100) (c) and (110) (d) parallel to substrates, as masks. The insets in (c) and (d) show the schematic depiction of formation of Au patterns by templating with (100) and (110) facets. Reprinted with permission.[74]

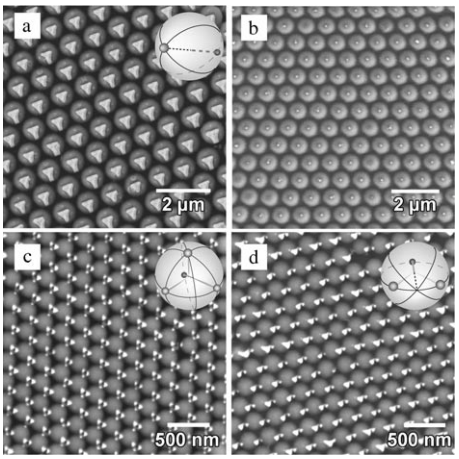

Figure 10. (a) SEM image of the gold patterns deposited on the upper halves of 925 nm PS spheres in the third layer obtained by using their colloidal crystals, etched by O_2 plasma for 10 min, as templates. (b) SEM image of the Au patterns obtained on the lower halves of these spheres. (c and d) SEM images of the gold Au patterns on the upper halves of 270 nm PS spheres by using their colloidal crystals, etched by O_2 plasma for 3 min, as templates constructed. The incidence angle of gold vapor is 0° (c) and 10° (d). The insets are the schematic illustration of the spatial configuration of gold nanodots decorated on the microspheres. Reprinted with permission.[75]

such as plasma etching time and the incidence angle of the vapor beam, also show a clear influence of the pattern feature deposited on the microspheres.[76] Pawar and Kretzschmar have recently demonstrated a new—less sophisticated but simpler—technique to pattern microspheres by deposition of gold on an hcp single layer of microspheres at a glancing incidence angle ($\theta > 60°$).[77] The pattern formation is the result of a shadow mask effect of neighboring microspheres under glancing incidence of the vapor beam.

In addition to the masking from a single layer or a double layer, an hcp multilayer of microspheres have also been employed for deposition of patterning microspheres. In order to suppress non-uniform vapor diffusion through the interstices in the upper double layers, the multilayer is etched by O_2 plasma prior to deposition. After gold vapor deposition, followed by peeling off the upper two layers with a sticky stamp, one, two, three, or four gold nanodots are decorated on the surface of the third layer exposed directly to the vapor beam (Figure 10).[75] The number of the gold dots obtained is dependent on the crystal structure including crystalline face and stacking symmetry, and the incidence angle of the vapor beam. Intriguingly, when more than three layers are used for deposition, there is another small round dot on the side of the third layer spheres opposite to the vapor beam, which is expected because of the scattering of the vapor by the lower layer spheres and the substrate (Figure 10b).[75] Taking the gold nanodots decorated on a microsphere as a whole, their configurations resemble those of S and P hybridized atomic orbitals embodied in carbon or silicon. In this scenario, the gold nanodots should be regarded as nanoscale valences to direct the spatial coupling between the decorated microspheres and thus realize hierarchical particle clusters with a supramolecular structural complexity.[78]

2.4. Extension of Colloidal Lithography

The patterns both on planar substrates and on microspheres, derived from colloidal crystal masking, create a clear-cut chemical heterogeneity on the surfaces. This encourages one to use them as masks for etching the supporting substrates or as seeds for growing different materials. Kuo and co-workers have used gold dots, obtained by double-layer-masked CL, as masks for etching silicon wafers by using a reactive ion beam, and fabricated a hexagonal array of silicon nanopillars with a diameter as small as 40 nm and aspect ratio as high as seven.[79] By etching silicon wafers in the presence of an hcp single microsphere layer atop, Weekes and co-workers have fabricated a non-close-packed hexagonal array of magnetic nanodots.[80] On the other hand, regular arrays of metallic nanodots derived from CL have been used as seeds for the growth of regular arrays of various nanotubes, nanorods, and nanowires with the aid of more sophisticated deposition techniques, such as plasma-enhanced chemical vapor deposition and molecular beam epitaxy.[81–85] With the aid of CL, large-area, hexagonally-arranged, highly-aligned carbon nanotubes and ZnO nanorods have been constructed, demonstrating the possibility of constructing devices from nanorods (Figure 11).[83,85] Mulvaney and co-workers have succeeded in creating a lateral superlattice structure of quantum dots on gold patterns derived from CL by alternative deposition of the quantum dots and alkanedithiol molecules.[86] These recent extensions of CL largely widen the application spectrum of CL and endorse the significance of CL on surface patterning.

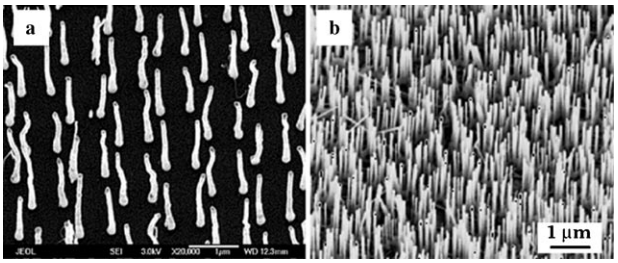

Figure 11. (a) SEM image of the highly ordered hexagonal array of aligned carbon nanotubes grown by plasma-enhanced chemical vapor deposition. Hexagonally arranged nickel dots obtained on a silicon wafer by CL are used as seeds. Reprinted with permission.[83] (b) SEM image of the highly ordered hexagonal array of aligned ZnO nanorods obtained by vapor-liquid-solid growth. Hexagonally arranged gold dots obtained on a single crystal alumina substrate by CL are used as seeds. Reprinted with permission.[85]

3. Conclusive Remarks and Future Challenges

The recent development of CL, especially the integration of etching the colloidal mask, altering the incidence angle, and stepwise and regular changing of the mask registry, leads to a powerful nanochemical patterning tool with low cost in capital and operation, high throughput, and ease for adoption on various planar and curved surfaces and even on microparticles. In difference from conventional mask-assisted lithographic processes, in which the mask design and production usually remain a challenge for scaling down the feature size and diversifying the feature shape, CL embodies a simple way for masking—self-assembly of monodisperse microspheres on a targeted substrate. The feature size can easily shrink below 100 nm by reducing the diameter of the microspheres used according to the simple correlation between the interstice size and the sphere diameter. The feature shape can be easily diversified by the crystalline structure of a colloidal crystal mask, the time of anisotropic etching of the mask, the incidence angle of the vapor beam and the mask registry (the azimuth angle of the vapor beam). Currently, CL allows fabrication of very complicated 2D and 3D nanostructured features, such as multiplex nanostructures with a clear-cut lateral and vertical heterogeneity. A number of new nanostructures are hard to be implemented, or cannot be in some cases, by conventional lithographic techniques. As such, CL provides a nanochemical and complementary tool for conventional and fully top-down lithographic techniques, and thus holds immense promise in surface patterning.

However, CL is still in a very early stage of development. Despite the great progress in colloidal crystallization it still remains a formidable challenge to create a defect-free single crystal with a defined crystalline face. The presence of defects dramatically reduces the patterning precision of CL. For instance, the random orientation of crystalline domains in a colloidal mask is a disaster for collimating the mask registry. In this aspect, template-assisted epitaxy for colloidal crystallization is promising as it allows growth of colloidal crystals with defined packing structure and orientation. Since a patterned substrate is necessitated for colloidal epitaxy, its applicability for patterning is limited. The transfer of a colloidal crystal derived from this colloidal epitaxy onto different substrates without deterioration of the crystal quality should be an ensuing task for CL. Besides, fabrication of a large area monolayer of periodically close-packed microspheres with sizes smaller than 100 nm remains significantly challenging, which brings a technical problem to reduce the feature size below 10 nm using CL. In a CL patterning process, furthermore, the feature size and the interspace size between the features cannot be separately manipulate, as they both are directly proportional to the sphere size in a colloidal mask, which largely limits the patterning capability of CL.

Arising from the processing simplicity and ease of accessibility, CL is extensively used by chemists, biochemists, and some physicists, and occasionally by microelectronic engineers. As a newly-developing patterning technique, CL should become an important addition to micro- and nanofabrication. However, there remains doubt on how to integrate CL with the diverse state-of-the-art lithographic techniques developed thus far and how to integrate the CL process or colloidal crystal masking for the microfabrication of a device. How well one can develop new technical ingenuity to overcome these major challenges will determine the fate and impact of CL on microfabrication.

Acknowledgements

We thank the Max Planck Society for the financial support. G.Z. thanks the NSFC for the financial support (No. 50703015).

[1] An opinion on semiconductor manufacturing development: W. M. Adrden, *Curr. Opin. Solid State Mater. Sci.* **2002**, *6*, 371–377.
[2] A survey of micro- and nanofabrication techniques: A. del Campo, E. Arzt, *Chem. Rev.* **2008**, *108*, 911–945.
[3] A review on new development of surface patterning: M. Geissler, Y. Xia, *Adv. Mater.* **2004**, *16*, 1249–1269.
[4] A review on photolithography: S. Okazaki, *J. Vac. Sci. Technol. B* **1991**, *9*, 2829–2833.
[5] A review on interference lithography: J. H. Moon, J. Ford, S. Yang, *Polym. Adv. Technol.* **2006**, *17*, 83–93.
[6] A review on nanoimprinting: H. Schift, *J. Vac. Sci. Technol. B* **2008**, *26*, 458–480.
[7] A review on multiphoton microfabrication: S. Maruo, J. T. Fourkas, *Laser Photonics Rev.* **2008**, *2*, 100–111.
[8] A review on probe-related patterning: D. Wouters, U. S. Schubert, *Angew. Chem.* **2004**, *116*, 2534–2550; *Angew. Chem. Int. Ed.* **2004**, *43*, 2480–2495.
[9] A review on electron beam lithography: J. M. Gibson, *Phys. Today* **1997**, 56–61.
[10] A review on dip-pen writing: D. S. Ginger, H. Zhang, C. A. Mirkin, *Angew. Chem.* **2004**, *116*, 30–46; *Angew. Chem. Int. Ed.* **2004**, *43*, 30–45.
[11] G. M. Whitesides, *Nat. Biotechnol.* **2003**, *21*, 1161–1165.
[12] P. Ball, *Nachr. Chem.* **2004**, *52*, 131–136.
[13] G. Ozin, A. Arsenault, *Nanochemistry: A Chemical Approach to Nanomaterials*, Royal Society of Chemistry, **2005**, London.
[14] J. Shen, J. Kirschner, *Surf. Sci.* **2002**, *500*, 300–322.
[15] Y. Xia, J. A. Rogers, K. E. Paul, G. M. Whitesides, *Chem. Rev.* **1999**, *99*, 1823–1848.

[16] Y. Xia, G. M. Whitesides, *Angew. Chem.* **1998**, *110*, 568–594; *Angew. Chem. Int. Ed.* **1998**, *37*, 550–575.
[17] I. W. Hamley, *Angew. Chem.* **2003**, *115*, 1730–1752; *Angew. Chem. Int. Ed.* **2003**, *42*, 1692–1712.
[18] J. V. Barth, G. Costantini, K. Kern, *Nature* **2005**, *437*, 671–679.
[19] X. Chen, S. Lenhert, M. Hirtz, N. Lu, H. Fuchs, L. Chi, *Acc. Chem. Res.* **2007**, *40*, 393–401.
[20] X. Zhang, A. V. Whitney, J. Zhao, E. M. Hicks, R. P. Van Duyne, *J. Nanosci. Nanotechnol.* **2006**, *6*, 1–15.
[21] N. C. Seeman, A. M. Belcher, *Proc. Natl. Acad. Sci. USA* **2002**, *99*, 6451–6455.
[22] Y. Xia, B. Gates, Y. Yin, Y. Liu, *Adv. Mater.* **2000**, *12*, 693–713.
[23] C. Lopez, *Adv. Mater.* **2003**, *15*, 1697–1704.
[24] D. Wang, H. Möhwald, *J. Mater. Chem.* **2004**, *14*, 459–468.
[25] A. Arsenault, S. Fournier-Bidoz, B. Hatton, H. Míguez, N. Tétreault, E. Vekris, S. Wong, S. M. Yang, V. Kitaev, G. A. Ozin, *J. Mater. Chem.* **2004**, *14*, 781–794.
[26] U. Ch. Fischer, H. P. Zingsheim, *J. Vac. Sci. Technol.* **1981**, *19*, 881–885.
[27] H. W. Deckmann, J. H. Dunsmuir, *Appl. Phys. Lett.* **1982**, *41*, 377–379.
[28] H. W. Deckmann, J. H. Dunsmuir, *J. Vac. Sci. Technol. B* **1983**, *1*, 1109–1112.
[29] H. W. Deckmann, J. H. Dunsmuir, S. Garoff, J. A. MaHenny, D. G. Peiffer, *J. Vac. Sci. Technol. B* **1988**, *6*, 333–336.
[30] J. C. Hulteen, R. P. Van Duyne, *J. Vac. Sci. Technol. A* **1995**, *13*, 1553–1558.
[31] J. C. Hulteen, D. A. Treichel, M. T. Smith, M. L. Duval, T. R. Jensen, R. P. Van Duyne, *J. Phys. Chem. B* **1999**, *103*, 3854–3863.
[32] C. L. Haynes, R. P. Van Duyne, *J. Phys. Chem. B* **2001**, *105*, 5599–5611.
[33] C. L. Haynes, A. D. McFarland, M. T. Smith, J. C. Hulteen, R. P. Van Duyne, *J. Phys. Chem. B* **2002**, *106*, 1898–1902.
[34] T. R. Jensen, M. D. Malinsky, C. L. Haynes, R. P. Van Duyne, *J. Phys. Chem. B* **2000**, *104*, 10549–10556.
[35] K. A. Willets, R. P. Van Duyne, *Annu. Rev. Phys. Chem.* **2007**, *58*, 267–297.
[36] P. Jiang, J. F. Bertone, K. S. Hwang, V. L. Colvin, *Chem. Mater.* **1999**, *11*, 2132–2140.
[37] Z.-Z. Gu, A. Fujishima, O. Sato, *Chem. Mater.* **2002**, *14*, 760–765.
[38] D. Wang, H. Möhwald, *Adv. Mater.* **2004**, *16*, 244–247.
[39] P. Jiang, M. J. Mcfarlan, *J. Am. Chem. Soc.* **2005**, *127*, 3710–3711.
[40] F. Garcia-Santamaria, H. T. Miyazaki, A. Urquia, M. Ibisate, M. Belmonte, N. Shinya, F. Meseguer, C. Lopez, *Adv. Mater.* **2001**, *14*, 1144–1147.
[41] A. van Blaaderen, R. Ruel, P. Wiltzius, *Nature* **1997**, *385*, 321–324.
[42] Y. Yin, Y. Xia, *Adv. Mater.* **2002**, *14*, 605–608.
[43] V. Kitaev, G. A. Ozin, *Adv. Mater.* **2003**, *15*, 75–78.
[44] S. Reculusa, S. Ravaine, *Chem. Mater.* **2003**, *15*, 598–605.
[45] Z.-Z. Gu, D. Wang, H. Möhwald, *Soft Matter* **2007**, *3*, 68–70.
[46] B. Gates, D. Qin, Y. Xia, *Adv. Mater.* **1999**, *11*, 466–469.
[47] A. Kosiorek, W. Kandulski, H. Glaczynska, M. Giersig, *Small* **2005**, *1*, 439–444.
[48] D. Choi, H. K. Yu, S. G. Jang, S. M. Yang, *J. Am. Chem. Soc.* **2004**, *126*, 7019–7025.
[49] J. H. Moon, S. G. Jang, J.-M. Lim, S.-M. Yang, *Adv. Mater.* **2005**, *17*, 2559–2562.
[50] J. G. C. Veinot, H. Yan, S. M. Smith, J. Cui, Q. Huang, T. J. Marks, *Nano Lett.* **2002**, *2*, 333–335.
[51] Y. Lu, G. L. Liu, J. Kim, Y. X. Mejia, L. P. Lee, *Nano Lett.* **2005**, *5*, 119–124.
[52] A. Kosiorek, W. Kandulski, P. Chudzinski, K. Kempa, M. Giersig, *Nano Lett.* **2004**, *4*, 1359–1363.
[53] G. Zhang, D. Wang, *J. Am. Chem. Soc.* **2008**, *130*, 5616–5617.
[54] G. Zhang, D. Wang, H. Möhwald, *Nano Lett.* **2007**, *7*, 3410–3413.
[55] G. Zhang, D. Wang, H. Möhwald, *Nano Lett.* **2007**, *7*, 127–132.
[56] A. N. Goldstein, C. M. Echer, A. P. Alivisatos, *Science* **1992**, *256*, 1425–1427.
[57] A. Habenicht, M. Olapinski, F. Burmeister, P. Leiderer, J. Boneberg, *Science* **2005**, *309*, 2043–2045.
[58] J. Yao, X. Yan, G. Lu, K. Zhang, X. Chen, L. Jiang, B. Yang, *Adv. Mater.* **2004**, *16*, 81–84.
[59] X. Yan. J. Yao, G. Lu. X. Chen, K. Zhang, B. Yang, *J. Am. Chem. Soc.* **2004**, *126*, 10510–10511.
[60] X. Yan, J. Yao, G. Lu, X. Li, J. Zhang, K, Han, B. Yang, *J. Am. Chem. Soc.* **2005**, *127*, 7688–7689.
[61] S. M. Yang, G. A. Ozin, *Chem. Commun.* **2000**, 2507–2508.
[62] K. Yamazaki, H. Namatsu, *Microelectron. Eng.* **2004**, *73–74*, 85–89.
[63] M. Albrecht, G. Hu, I. L. Guhr, T. C. Ulbrich, J. Boneberg, P. Leiderer, G. Schatz, *Nat. Mater.* **2005**, *4*, 203–206.
[64] H. Takei, N. Shimizu, *Langmuir* **1997**, *13*, 1865–1868.
[65] L. Petit, E. Sellier, E. Duguet, S. Ravaine, C. Mingotaud, *J. Mater. Chem.* **2000**, *10*, 253–254.
[66] D. R. Nelson, *Nano Lett.* **2002**, *2*, 1125–1129.
[67] Z. Zhang, S. C. Glotzer, *Nano Lett.* **2004**, *4*, 1407–1413.
[68] Z. Zhang, A. S. Keys, T. Chen, S. C. Glotzer, *Langmuir* **2005**, *21*, 11547–11551.
[69] D. G. Shchukin, D. S. Kommireddy, Y. Zhao, T. Cui, G. B. Sukhorukov, Y. M. Lvov, *Adv. Mater.* **2004**, *16*, 389–393.
[70] L. Hong, A. Cacciuto, E. Luijten, S. Granick, *Nano Lett.* **2006**, *6*, 2510–2514.
[71] C. E. Snyder, A. M. Yake, J. D. Feick, D. Velegol, *Langmuir* **2005**, *21*, 4813–4815.
[72] Z. Bao, L. Chen, M. Weldon, E. Chandross, O. Cherniavskaya, Y. Dai, J. B. H. Tok, *Chem. Mater.* **2002**, *14*, 24–26.
[73] V. N. Paunov, O. J. Cayre, *Adv. Mater.* **2004**, *16*, 788–791.
[74] G. Zhang, D. Wang, H. Möhwald, *Nano Lett.* **2005**, *5*, 143–146.
[75] G. Zhang, D. Wang, H. Möhwald, *Angew. Chem.* **2005**, *117*, 7945–7948; *Angew. Chem. Int. Ed.* **2005**, *44*, 7767–7770.
[76] G. Zhang, D. Wang, H. Möhwald, *Chem. Mater.* **2006**, *18*, 3985–3992.
[77] A. B. Pawar, I. Kretzschmar, *Langmuir* **2008**, *24*, 355–358.
[78] E. W. Edwards, D. Wang, H. Möhwald, *Macromol. Chem. Phys.* **2007**, *208*, 439–445.
[79] C. W. Kuo, J.-Y. Shiu, P. Chen, G. A. Somorjai, *J. Phys. Chem. B* **2003**, *107*, 9950–9953.
[80] S. M. Weekes, F. Y. Ogrin, W. A. Murray, *Langmuir* **2004**, *20*, 11208–11212.
[81] B. Fuhrmann, H. S. Leipner, H.-R. Höhe, L. Schubert, P. Werner, U. Gösele, *Nano Lett.* **2005**, *5*, 2524–2527.
[82] C. K. Tan, K. P. Loh, J. T. L. Thong, C. H. Sow, H. Zhang, *Diamond Relat. Mater.* **2005**, *14*, 902–906.
[83] K. Kempa, B. Kimball, J. Rybczynski, Z. P. Huang, P. F. Wu, D. Steeves, M. Sennett, M. Giersig, D. V. G. L. N. Rao, D. L. Canahan, D. Z. Wang, J. Y. Lao, W. Z. Li, Z. F. Ren, *Nano. Lett.* **2003**, *3*, 13–18.
[84] J. Rybcynski, D. Banerjee, A. Kosiorek, M. Giersig, Z. F. Ren, *Nano Lett.* **2004**, *4*, 2037–2040.
[85] X. Wang, C. J. Summers, Z. L. Wang, *Nano Lett.* **2004**, *4*, 423–426.
[86] J. Pacifico, J. Jasieniak, D. E. Gomez, P. Mulvaney, *Small* **2006**, *2*, 199–203.

Received: October 1, 2008
Published online: November 5, 2008

